Bull. Mater. Sci., Vol. 17, No. 1, February 1994, pp. 59–72. © Printed in India.

The role of additives in a complex lithium silicate glass-ceramic#

R N DAS†, B K CHANDRASEKHAR† and K J RAO*
Materials Research Centre, Indian Institute of Science, Bangalore 560012, India
†Ceramic Technological Institute, Bharat Heavy Electricals Ltd, Bangalore 560012, India

MS received 13 January 1994

Abstract. Several glass-ceramic compositions based on lithium silicates have been examined using thermal expansivity, X-ray diffraction, electrical conductivity, electron microscopy and solid state NMR studies. Role of P_2O_5 in nucleation and of Al_2O_3 in smoothening expansion behaviour have been particularly highlighted. Magic angle spinning NMR has been used to ascertain presence of Al in tetrahedral positions in the glassy phase.

Keywords. Glass-ceramic; lithium silicates; nucleation; minor additives; thermal expansivity; sealing; MASNMR.

1. Introduction

One of the important and large-volume industrial applications of glasses has been in glass-to-metal seals. It has been known for a long time that silicate glasses containing lithia are particularly useful for glass-to-steel seals. These glasses crystallize at an easily accessible temperature and give rise to a glass-ceramic consisting of lithium disilicate (Borom *et al* 1975; McCollister and Reed 1983; Haws *et al* 1986; Loehman and Headley 1987; Cassidy and Moddeman 1989; Moddeman *et al* 1989). The presently used sealing glass compositions contain several additives such as alumina, phosphorous pentoxide and alkali oxides, and understanding of the role of such additives requires further investigation. For example the structural role of P_2O_5 as nucleating agent and the mechanism of action of Al_2O_3 in smoothing out thermal strains during partial ceramization are still unclear. Special schedules of thermal treatment are also in vogue in the applications of lithia-based silicate glass-ceramics (Borom *et al* 1975; McCollister and Reed 1983; Headley and Loehman 1984; Haws *et al* 1986; Moddeman *et al* 1989), and it would be interesting to understand the critical role of such heat treatment schedules. We therefore feel that it is important to investigate in detail this industrial glass-ceramic in order to appreciate clearly the role of the additives and the importance of the thermal histories accorded to glass-ceramics in their applications. In this communication we present results of our studies on several glasses chosen so as to comprise most of the currently employed glass-ceramic compositions suitable for glass-to-steel sealing applications. Our investigations include extensive thermal expansivity measurements, X-ray diffractometry, electron microscopy, measurement of ultrasound velocities and high-resolution magic angle spinning NMR spectroscopy (MASNMR) of ^{29}Si, ^{27}Al and ^{31}P.

#Communication number 164 from Materials Research Centre
*For correspondence

Table 1. Glass batch compositions.

	Composition in mol% (wt% in parentheses)						
	Composition no.						
Component	I	II	CTI1	CTI2	CTI3	CTI4	Range
SiO_2	74·27 (82·04)	73·94 (81·01)	74·40 (82·19)	74·18 (81·74)	73·61 (80·58)	71·91 (78·29)	71·91–74·40 (78·29–82·19)
Li_2O	23·02 (12·65)	22·92 (12·49)	23·06 (12·67)	22·99 (12·60)	22·82 (12·42)	23·40 (12·67)	22·82–23·40 (12·42–12·67)
K_2O	1·51 (2·61)	1·50 (2·58)	1·69 (2·93)	1·69 (2·92)	1·67 (2·87)	1·72 (2·93)	1·50–1·72 (2·58–2·93)
P_2O_5	0·60 (1·57)	1·20 (3·10)	0·85 (2·21)	0·84 (2·20)	0·84 (2·17)	0·86 (2·21)	0·60–1·20 (1·57–3·10)
Al_2O_3	0·60 (1·13)	0·44 (0·83)	0·00 (0·00)	0·29 (0·55)	1·06 (1·96)	2·11 (3·91)	0·00–2·11 (0·00–3·91)

2. Experimental

The glass compositions indicated in table 1 were prepared in 100 g batches by mixing reagent-grade K_2HPO_4 (AR; Loba Chemie, Bombay), Li_2CO_3 (minimum 99% purity; Lithium Chemicals & Products, Calcutta), quartz (minimum 99.5% SiO_2) and alumina (minimum 99% Al_2O_3, HTM grade; Indian Aluminum Co., Belgaum) in an agate mortar for a few hours. The mix was put in a platinum crucible and heated to 1450°C for 18 h in air in an electrically heated furnace. After melting, the glass was cast into discs and rods of 5 mm diameter which were later cut and polished to get 50-mm-long rods for the measurements of thermal expansion and other properties.

All the glass rods were annealed at 430°C for 2 h. Glasses I and II were nucleated at various temperatures ranging from 465°C to 540°C for various durations of time. Other glasses were nucleated at 520°C for 95 min. The heat treatment was carried out in air in an electrically heated furnace. All the nucleated glasses were crystallized at 847 ± 2°C and the rate of heating was set at 10°C/min on a microprocessor-controlled heat-treatment furnace.

All the thermal expansion measurements were carried out by using both horizontal model TDA-H1-PP6, Harrop Industries Inc., Columbus, USA and vertical model TDA-V3-5, Harrop push rod dilatometers at fixed rate of heating.

The as-quenched, nucleated and devitrified glasses were characterized using an X-ray (CuK_α) powder diffractometer model D Max IIIA X-ray diffraction unit, Rigaku Denki Kogyo, Japan at room temperature.

Electron microscopic studies (TEM and SEM) of the samples were performed using a Philips EM301 transmission electron microscope for nucleated glass samples and a Cambridge S150 scanning electron microscope to investigate the microstructure of nucleated and devitrified glass samples polished mechanically and etched by dilute hydrofluoric acid.

Electrical conductivities of the glasses were studied both as a function of temperature (room temperature to 250°C) and frequency (30 Hz–100 kHz) using a GR 1608A

Table 2. NMR parameters used in this study.

Nucleus	Resonance frequency (MHz)	Pulse width (μs)	Delay time (s)	Spectral width (kHz)	Spinning speed (kHz)	Standard
^{29}Si	59·621	5	500	25	~3	TMS
^{27}Al	78·206	0·7	0·1	125	~3	$[Al(H_2O)_6]^{3+}$
^{31}P	121·494	5	5	125	~3	85% H_3PO_4

(General Radio, USA) impedance bridge on discs of 11 mm diameter and 4 mm thickness. The silver coatings on both sides of the sample served as reversible electrodes. These silver coatings were removed completely to avoid silver diffusion before carrying out any heat treatment of the samples.

^{29}Si, ^{31}P and ^{27}Al MASNMR spectra were recorded with a solid-state high-resolution Bruker MSL-300 spectrometer according to the conditions summarized in table 2.

Ultrasonic velocity measurements were performed at 10 MHz, using quartz X and Y cut transducers (Bharat Electronics Ltd., Bangalore) by McSkimin's pulse superposition method (McSkimin 1961). Salol (phenyl salicylate) was used as the bonding material. A pulsed oscillator Arenberg PG-650C, Arenberg Ultrasonic Lab. Inc., Boston and an ultrasonic pulse echo interferometer (Systems Dimensions, Bangalore) were used for the velocity measurements.

3. Results and discussion

3.1 *Nucleation studies*

It is established in the literature (Borom *et al* 1975) that nucleation of crystalline lithium silicate phases begins to be manifest at temperatures above 450°C. We have therefore chosen four different temperatures (T_n) for our nucleation studies. Various compositions investigated in our studies are listed in table 1. In particular, compositions I and II are very similar except for the differences in P_2O_5 content; the concentration of P_2O_5 in glasses I and II is in the ratio 1:2. We give in figure 1 variation of $\delta L/L$ for the glass composition I which was subjected to nucleation at four different tem-

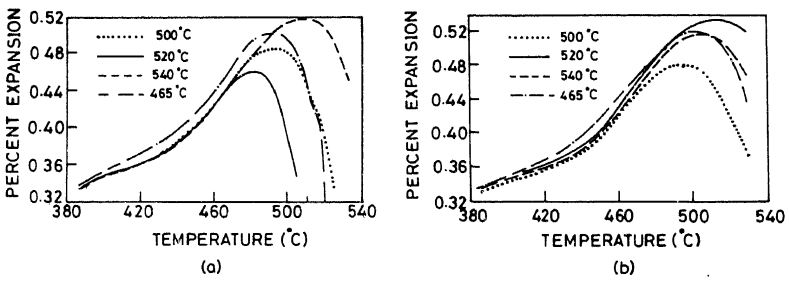

Figure 1. Linear thermal expansion behaviour of glass I nucleated at indicated temperatures for (**a**) 1 h and (**b**) 5 h. Rate of heating during the expansion measurement: 2°C/min.

peratures and for two different periods of time. The marked decrease in $\delta L/L$ value indicates the onset of rapid deformation of the samples under the experimental spring load and hence it corresponds to dilatometric softening temperature, $T_g(d)$.

An important observation from figure 1 is that longer nucleation time increases the dilatometric softening temperature; also, the effect of nucleation is most pronounced for $T_n = 520°C$. The softening temperature increases from 480°C to 510°C (reckoned from peak positions) as the nucleation holding time is increased from 1 to 5 h. Although nucleation at 540°C seems to require less time for attaining maximum dilatometric softening temperature, longer holding times only seem to decrease $T_g(d)$. Similar behaviour was observed for glass composition II also, in which the P_2O_5 content was twice as high. The time required for nucleation, however, was seen to be far lower. Typical plots are shown in figure 2.

Given in figure 3 are the coefficients of thermal expansion of glasses well below glass transition temperature. They were measured before and after nucleating them at various temperatures and for different holding times. The expansivities were found to be rather constant below 400°C for these glasses. Expansivities were determined by regression analysis which gave a correlation $r^2 > 0{\cdot}998$ for each individual plot. It may be noted from figure 3 that expansivities marginally decreased as the nucleation hold times were increased. At nucleation temperature of 500°C and above, expansivity decreases initially for hold times of under one hour, and the variation is rather insignificant above this time. The initial differences in expansivities of about 2·5% for samples nucleated at different temperatures may arise from limitations inherent to this type of measurement.

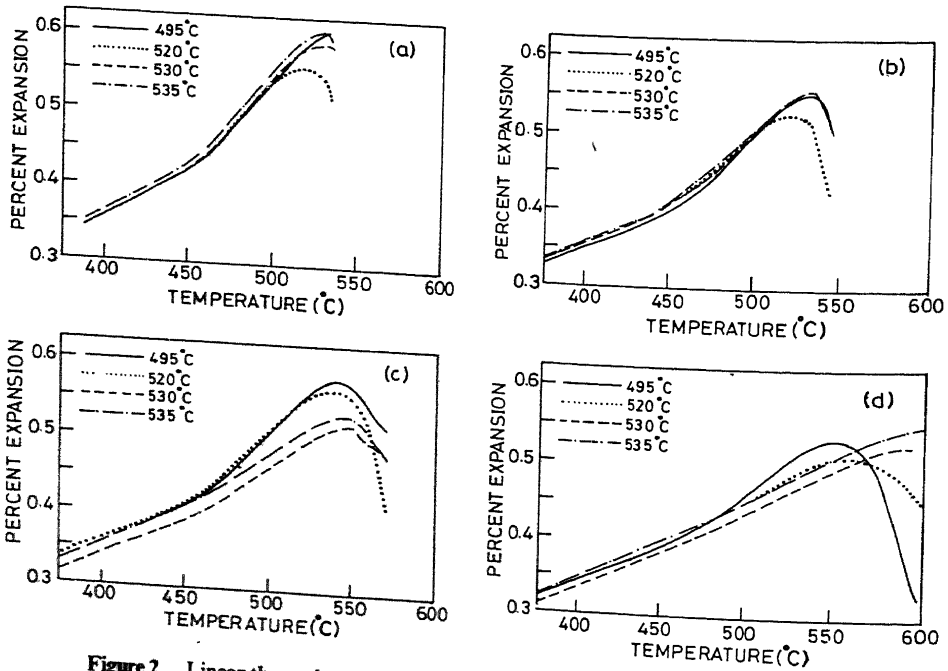

Figure 2. Linear thermal expansion behaviour of glass II nucleated at indicated temperatures for (a) 10 min, (b) 20 min, (c) 40 min and (d) 60 min. Rate of heating during the expansion measurement: 10°C/min.

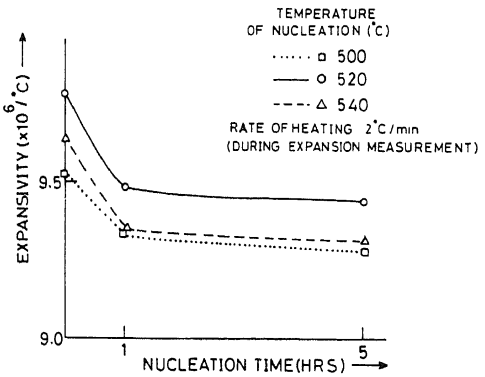

Figure 3. Coefficient of thermal expansion of glass I below glass transition temperature as a function of nucleation heat treatment time.

Taken together, figures 1, 2 and 3 imply the following. At the nucleation stage lithium monosilicate nuclei (see later) are formed, rendering the matrix relatively rich in silica. As expected, phosphate groups would all be involved in nucleation and hence associated with lithium monosilicate nuclei. These nuclei have an average size which depends on the nucleation temperature and the sizes are evidently larger for higher nucleation temperatures. The rheological behaviour of the resulting micro-heterogeneous (crystalline nuclei plus the glassy matrix) mixtures is dependent on the extent of nuclei–matrix interface and the viscosity of the matrix which is the continuous phase. In the present case the matrix is slightly richer in silica, hence has higher viscosity. The combined influence of these two factors, namely sizes of the nuclei (high interface) and high viscosity, appears to give rise to a maximum dilatometric softening temperature, and the corresponding T_n is 520°C. Also, since the glass forms the continuous phase, the thermal expansivities of the nucleated glasses are essentially determined by the silica-rich glass phase, which are therefore nearly independent of both T_n and holding time.

The differential thermogram of a typical glass composition is shown in figure 4. Although the glass transition temperature itself is not very clearly evident in the thermogram the two crystallization temperatures are clearly exhibited. Presence of two crystallization temperatures is a common feature (Hammetter and Loehman 1987) of all the glasses examined in this work. The first peak at 590°C corresponds to the formation of lithium monosilicate and we have confirmed this by XRD studies of a glass sample heated to only about 640°C (shown in the inset). It may be noted here that prior to the formation of disilicate the matrix viscosity decreases quite substantially (it is well above the glass transition temperature of the matrix). As seen in figure 5, this is evident from $\delta L/L$ versus temperature plot of the glass which was heated to 847°C and the deformation with the spring load on was examined. Around 520°C and up to around 740°C large decrease of $\delta L/L$ is seen. Beyond 740°C this trend not only stops but is reversed due to crystallization of the disilicate from the matrix glass.

The second crystallization peak corresponds to the formation of lithium disilicate. The melting transition (endotherm) following the second crystallization is evidently very diffuse because a silica-rich glass phase still remains in the glass-ceramic.

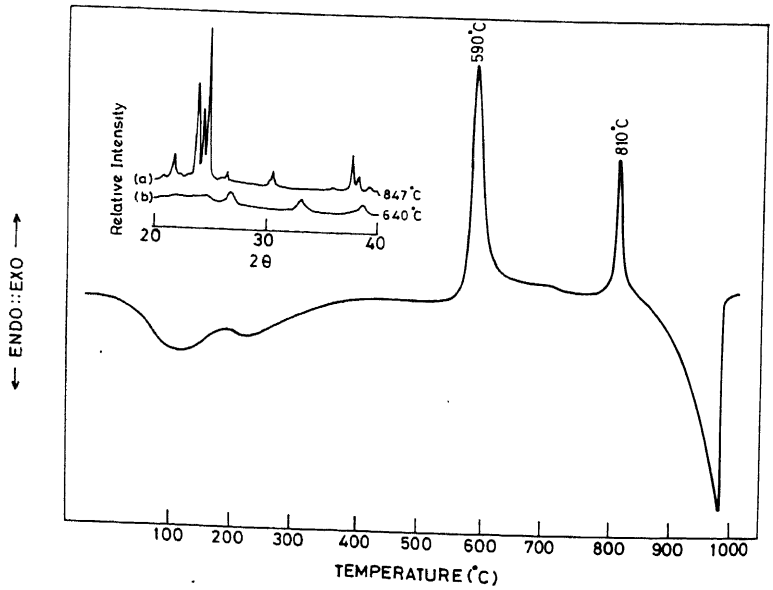

Figure 4. DTA trace at a heating rate of 10°C/min of as-cast glass I. In the inset XRD plots of the glass treated at (**a**) 847°C for 70 min and (**b**) 640°C for 60 min are shown, which confirm lithium monosilicate and lithium disilicate as the major phases respectively.

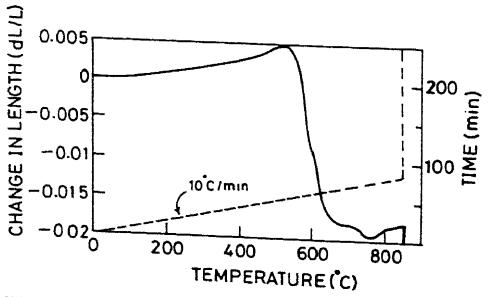

Figure 5. Change in length ($\delta L/L$) of the nucleated (95 min at 500°C) glass II rod as a function of temperature of heating at the rate of 10°C/min in a horizontal push rod dilatometer furnace and 220 min soaking after reaching 847°C.

Formation of lithium disilicate at the second crystallization was also confirmed by XRD studies as shown in the inset of figure 4. However, the X-ray diffraction pattern of the glass-ceramic contained, besides reflection from lithium disilicate, reflections due to cristoballite phase of SiO_2 also. During the formation of glass-ceramic the crystallites seem to grow to reasonably good sizes and are apparently not much influenced by the nucleation temperature and the hold time since full widths at half maximum (FWHM) of the X-ray diffraction peaks were found to be rather similar in all cases.

Nucleation of lithium silicate leaves the matrix glass-phase impoverished with respect to lithium ions and this seems to be reflected in a slight but definite drop in the conductivities of the nucleated glasses, as shown in figure 6. These conventional Arrhenius plots also suggest that a slight increase in the activation barrier occurs after nucleation.

3.2 *Role of alumina*

The most important aspect of our study in the context of technological application of this glass-ceramic is the effect of the addition of alumina to the glass. It appears to influence the rheology of the glass-ceramic at high temperatures. It is important in glass–metal seals that the expansivities of the glass-ceramic and the metal (e.g.

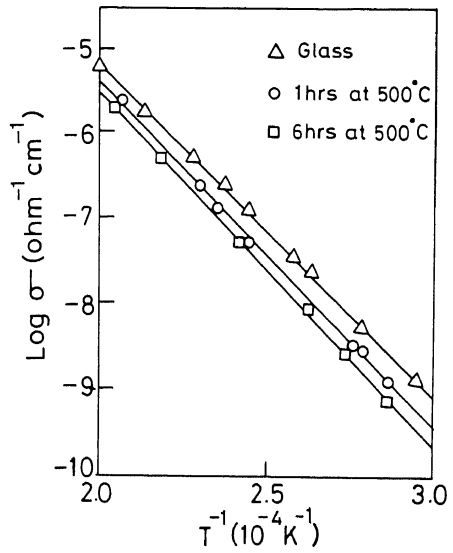

Figure 6. Arrhenius conductivity plot for glass I as a function of heat treatment time at $T_n = 500°C$.

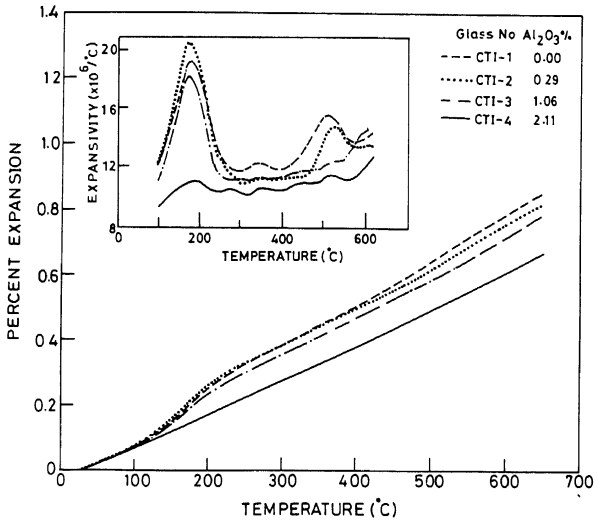

Figure 7. Dilatometric linear expansion traces (at 10°C/min heating rate) of crystallized glass nos. CTI1, CTI2, CTI3 and CTI4 with 0·0, 0·29, 1·06 and 2·11 mol% Al_2O_3 respectively. Expansivities (coefficients of thermal expansion) for the same glasses are plotted in the inset after smoothening the graph by taking running average of the expansivity at every 10°C interval.

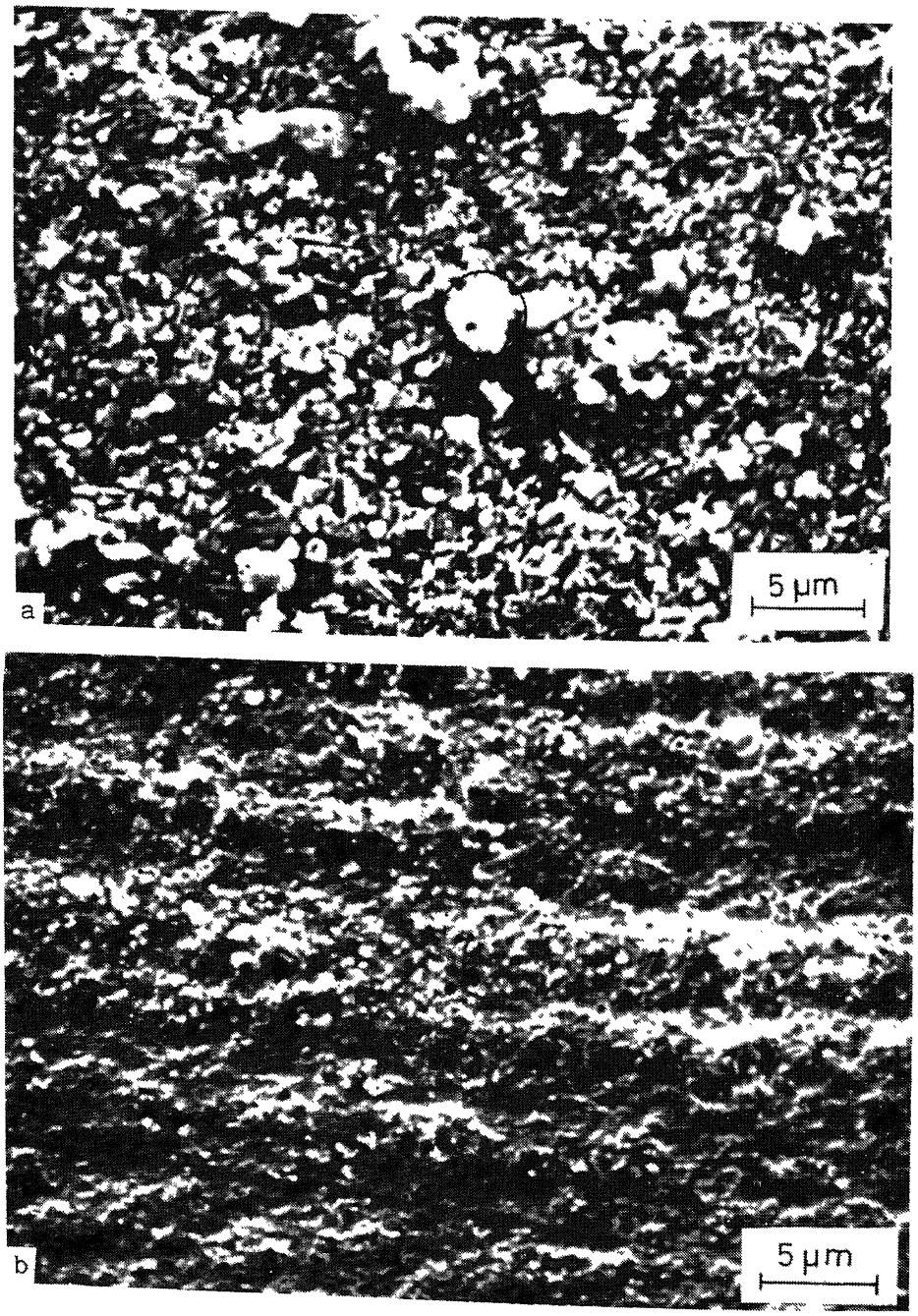

Figure 8. Scanning electron micrographs of fully crystallized glasses containing (**a**) 0·29 and (**b**) 2·11 mol% alumina. The encircled region in (**a**) shows one of the cristoballite particles.

steel) are well matched throughout the working range of temperatures. After crystallization glasses exhibit a small hump-like change around 170°C in linear expansion plots, as shown in figure 7 for glass nos. CTI1, CTI2, CTI3 and CTI4. This hump-like feature is manifested more clearly in expansivity plots shown in the inset. Somewhat

subdued peaks of expansivity occur in the region of 515°C also. These two peaks, around 170°C and around 515°C, may be tentatively associated with the α to β transformations of cristoballite and quartz respectively. It may be recalled here that during the crystallization quartz is also formed in small quantities. Addition of small amounts of alumina seems to suppress this feature, as is evident from figure 7, and makes the expansivity more compatible with the expansivities of various steels. It is well known that alumina readily dissolves in silica glass. Aluminium occupies tetrahedral position in the extended silicate network and is readily assisted by the presence of oxides like K_2O in this process (Prabhakar *et al*, 1992). Crystallization of quartz and cristoballite therefore requires exsolution of the dissolved alumina and hence a phase separation. This process is naturally hindered because vitreous phase is stabilized by random distribution of aluminium on silicon sites in the vitreous network. Hence cristoballite and quartz are not formed when sufficient quantity of alumina is present in the composition. We show later that the aluminium is indeed present only in tetrahedral positions in these glasses.

Evidence for the suppression of quartz and cristoballite formation when the alumina content is increased in the glass may be seen in electron micrographs presented in figure 8. The initial composition contains only 0·29 mol% alumina and in the resulting glass-ceramic cristoballite grains are easily recognized (figure 8a). In glasses containing 2·11 mol% Al_2O_3 no recognizable grains of cristoballite are seen (figure 8b).

3.3 *Elastic properties*

The nucleation of lithium silicates, however, could not be observed convincingly in electron microscopy even in samples soaked for a long time at the optimum nucleation temperature. In the diffraction patterns rings at distances relevant to monosilicate and disilicate were observed in some of our TEM samples. We expect the ultramicrostructure of the material after nucleation to be heterogeneous. Therefore elastic properties of such a material should be expected to register sensitive variations. We have therefore examined variations of ultrasound velocities (both longitudinal and shear) in glass I as a function of nucleation soak time. The variations are shown in figure 9, and in inset (a) variations of bulk modulus K and shear modulus G are also shown. The variations are indeed quite remarkable. The velocities increase monotonically as soak time increases or as nucleation of monosilicate phase increases. We have also given in inset (b) variation of the Grüneisen parameter γ calculated using literature values of heat capacity and other required parameters determined in this work. Various elastic properties and the input parameters are listed in table 3. Since the Grüneisen parameter $\gamma = \mathrm{d}\ln(\omega)/\mathrm{d}\ln(v)$, the observed variation in Grüneisen parameter suggests that some of the modes in silicate glasses vary in a manner typical of modified silicate glasses. Indeed the Grüneisen parameter has the same order of magnitude reported (Sato and Anderson 1980) for some of the alkali silicate glasses. It therefore suggests that elastic properties are quite sensitive to nucleation in glass-ceramics.

3.4 *NMR studies*

In the preceding section, we have noted that nucleation involving P_2O_5 is a critical step. Suppression of cristoballite formation is another important step. The latter

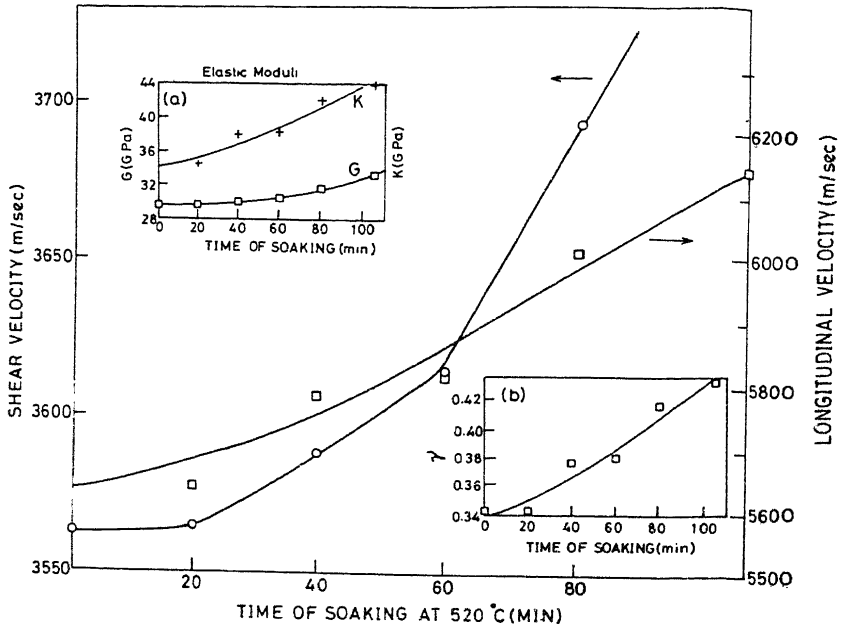

Figure 9. Ultrasound velocities (both longitudinal and shear) in glass I as a function of nucleation soak time. Variations of bulk and shear moduli are shown in inset (a). In inset (b) variation of Grüneisen parameter is shown.

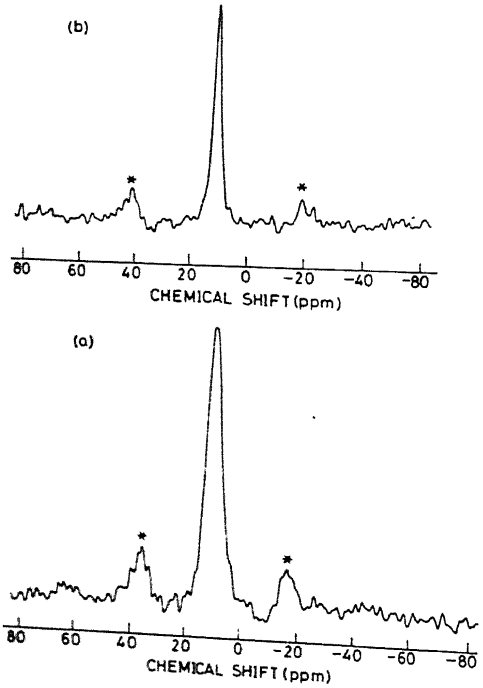

Figure 10. ^{31}P MASNMR spectra of (**a**) glass and (**b**) the crystallized glass-ceramics of composition no. CTI2. The asterisks on the peaks indicate spinning sidebands.

Table 3. Elastic properties of the nucleated glass.

Time of soak at 520°C (min)	Frequency		Velocity		Density (g/cm^3)	Molar volume (cm^3)	Shear modulus G (GPa)	Bulk modulus K (GPa)	Grüneisen constant
	Longitdn. (kHz)	Shear (kHz)	Longitdn. (m/sec)	Shear (m/sec)					
0	196·46	124·23	5634	3563	2·329	23·70	29·56	34·52	0·344
20	196·52	124·29	5636	3565	2·331	23·68	29·62	34·56	0·344
40	201·63	125·12	5783	3588	2·334	23·65	30·05	37·98	0·378
60	202·80	126·03	5816	3615	2·336	23·62	30·52	38·34	0·381
80	139·78	128·75	6013	3693	2·339	23·59	31·90	42·06	0·418
105	142·68	131·60	6138	3774	2·348	23·51	33·44	43·86	0·434

Sample thickness = 7·17 mm

Assumptions: Heat capacity (C_v) = 1·2267 joule/g/°C

Coefficient of thermal expansion (linear) = $9{\cdot}5 \times 10^{-6}$/°C

Molecular weight of the glass = 55·189

involves dissolution of alumina. It is vital to understand the nature of these phenomena at a molecular level. Since ^{27}Al, ^{29}Si and ^{31}P are all spin-bearing nuclei, they are conveniently studied by solid-state high-resolution MASNMR (Fyfe *et al* 1983; Prabhakar *et al* 1991).

In figure 10 we give the MASNMR spectra of ^{31}P in the glass CTI2 and in the crystallized glass-ceramic. In figure 11 MASNMR spectra of ^{31}P in the glass CTI4 before (figure 11a) and after (figure 11b) nucleation at 520°C for 95 min and in the corresponding glass-ceramic (figure 11c) are presented. It is quite evident that the NMR resonance which lies around 10 ppm is due to orthophosphate units (Dupree *et al* 1988; Prabhakar *et al* 1991). P_2O_5, being the most acidic oxide (Prabhakar *et al* 1991), is present entirely as orthophosphate ions in the glass. This charged anion along with Li^+ ions initially forms lithium orthophosphate which seems to be the real nucleating entity in the glass. Lithium orthophosphate itself being an ionic compound easily acquires a crystalline motif, as it is the predominant tendency in ionic materials. ^{29}Si spectrum itself indicates presence of both Q_3 and Q_4 units (Fyfe *et al* 1983; Prabhakar *et al*, communicated) in the freshly prepared glasses, as shown in figure 12a. Since the compositions are such that even after nucleation silica-rich glass phase is present in the medium the Q_4 resonances persist along with Q_3 from the monosilicate phase (spectra not shown). ^{27}Al NMR spectrum in the glass containing

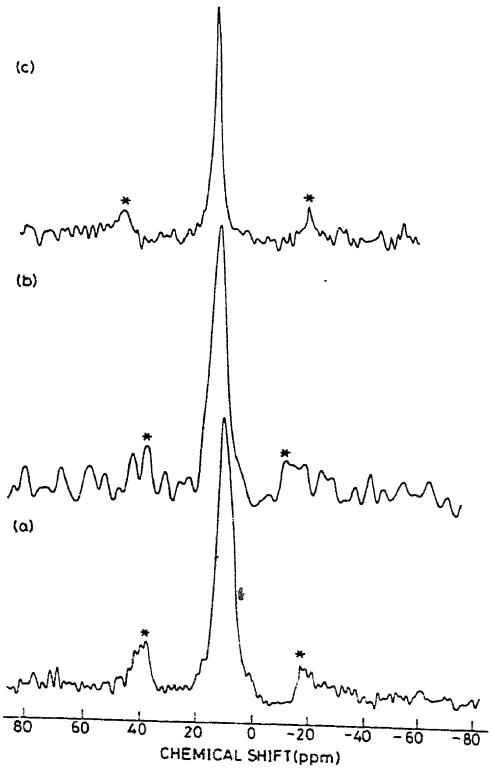

Figure 11. ^{31}P MASNMR spectra of (**a**) glass, (**b**) the nucleated glass (at 520°C for 95 min) and (**c**) the crystallized glass-ceramics of composition no. CTI4. The asterisks on the peaks indicate spinning sidebands.

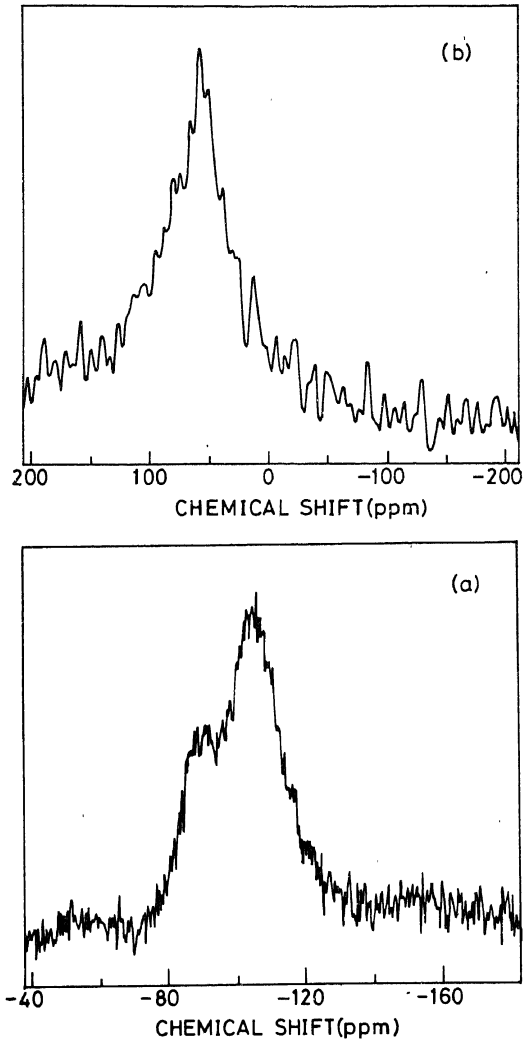

Figure 12. (a) ^{29}Si MASNMR spectrum of freshly prepared glass. (b) ^{27}Al MASNMR spectrum of the glass-ceramics (glass no. CTI4 after crystallization).

2·11 mol% Al_2O_3 is shown in figure 12b. It is indeed present in tetrahedral coordination as evident from its signal at 57·5 ppm. As pointed out earlier aluminium present in the vitreous silicate phase stabilizes the latter and hence suppresses formation of cristoballite.

4. Conclusions

This study has addressed two aspects of lithium disilicate-based glass-ceramics: firstly the optimum thermal history for nucleation, and secondly the role of alumina. It has been shown that the size of the nuclei which determines the nuclei–matrix interface and viscosity of the matrix of silicate glass establishes an optimum for temperature–

time treatment at the nucleation stage. Alumina plays the vital role of suppressing formation of cristoballite and quartz by dissolving in the vitreous phase of silica. Further, MASNMR has been used to show that the nucleation most likely involves formation of the crystalline lithium phosphates as a first stage.

Acknowledgements

The authors thank Dr K V Damodaran, Dr M C R Shastry, Dr S Prabhakar and Mr P V Satyasanda for extending cooperation in making several experimental measurements. We also thank Prof. C N R Rao, Mr B M R Rai and Mr L K Sachdeva for their kind encouragement.

References

Borom M P, Turkalo A M and Doremus R H 1975 *J. Am. Ceram. Soc.* **58** 385
Cassidy R T and Moddeman W E 1989 *Ceram. Eng. Sci. Proc.* **10** 1387
Dupree R, Holland D and Mortuza M G 1988 *Phys. Chem. Glasses* **29** 18
Fyfe C A, Thomas J M, Klinowski J and Gobbi G C 1983 *Angew. Chem. Int. Edn. Engl.* **22** 259
Hammetter W F and Loehman R E 1987 *J. Am. Ceram. Soc.* **70** 577
Haws L D, Kramer D P, Moddeman W E and Wooten G W 1986 US Dept of Energy Report No. MLM-3401/DE87 004040
Headley T J and Loehman R E 1984 *J. Am. Ceram. Soc.* **67** 620
Loehman R E and Headley T J 1987 in *Ceramic microstructure'86: The role of interfaces* (eds) J A Pask and A G Evans (New York: Plenum Press)
McCollister H L and Reed S T 1983 US Patent 4 414 282
McSkimin H J 1961 *J. Acoust. Soc. Am.* **33** 12
Moddeman W E, Pence R E, Massey R T, Cassidy R T and Kramer D P 1989 *Ceram. Eng. Sci. Proc.* **10** 1394
Prabhakar S, Rao K J and Rao C N R 1991 *J. Mater. Res.* **6** 592
Prabhakar S, Rao K J and Rao C N R 1992 *Eur. J. Solid State Inorg. Chem.* **29** 95
Sato Y and Anderson O L 1980 *J. Phys. Chem. Solids* **41** 401